Experimental Study of CO2, CH4, and Water Vapor Adsorption on a Dimethyl-Functionalized UiO-66 Framework

ARTICLE *in* THE JOURNAL OF PHYSICAL CHEMISTRY C · APRIL 2013

Impact Factor: 4.77 · DOI: 10.1021/jp311857e

2 AUTHORS, INCLUDING:

Himanshu Jasuja
Georgia Institute of Technology
16 PUBLICATIONS **476** CITATIONS

THE JOURNAL OF PHYSICAL CHEMISTRY C

Article

pubs.acs.org/JPCC

Experimental Study of CO_2, CH_4, and Water Vapor Adsorption on a Dimethyl-Functionalized UiO-66 Framework

Himanshu Jasuja and Krista S. Walton*

School of Chemical and Biomolecular Engineering, Georgia Institute of Technology, 311 Ferst Drive NW, Atlanta, Georgia 30332, United States

Supporting Information

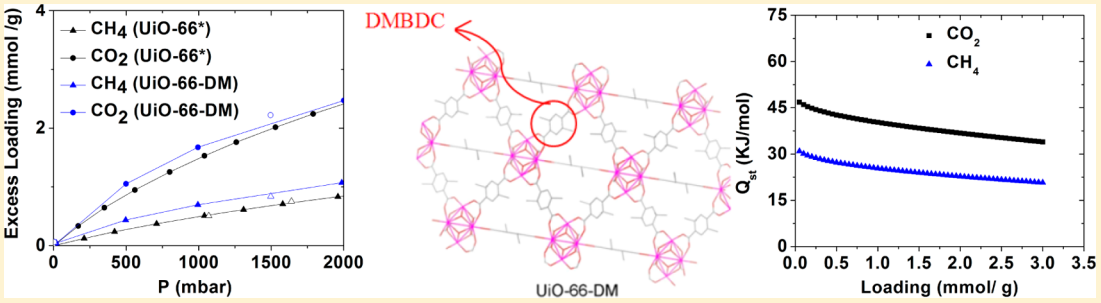

ABSTRACT: A water resistant, highly robust dimethyl-functionalized UiO-66 analogue (UiO-66-DM) has been synthesized and characterized by using N_2 adsorption, powder X-ray diffraction, ^{1}H nuclear magnetic resonance, Fourier transform infrared spectroscopy, and thermogravimetric analysis followed by mass spectroscopy. High-pressure (up to 20 bar) single-component adsorption isotherm measurements of CO_2 and CH_4 have been performed on UiO-66-DM at different temperatures (293−308 K). Adsorption isotherm data were modeled by using the Toth equation, and isosteric heats of adsorption were calculated by using the Clausius−Clapeyron equation. The Ideal Adsorbed Solution Theory (IAST) was used to calculate mixture selectivities. Water adsorption experiments show that water adsorption loadings in UiO-66-DM are reduced by almost 50% compared to the parent material. In the low-pressure region, functionalization of the benzenedicarboxylic ligand by 2,5-dimethyl leads to higher interactions with both CO_2 and CH_4 compared to the parent UiO-66. CO_2/CH_4 selectivity calculated from IAST is higher for UiO-66 in the low-pressure region (<5 bar) but for pressures >5 bar, UiO-66-DM is more CO_2 selective than UiO-66.

1. INTRODUCTION

The synthesis and characterization of porous materials for use as adsorbents and catalysts have been an active area of research for decades due to numerous uses in applications ranging from petrochemicals and catalysis to adsorption-based selective separations.[1] Traditional porous materials such as zeolites and similar oxide-based materials have been a focal point since 1960.[2] However, new developments in synthetic zeolites have been limited due to the relatively small size of the pores, difficulty in the tuning of these pores, and difficulty in chemical modification of the surface. Metal−organic frameworks (MOFs), which are made up of metal clusters linked to each other by organic ligands,[3] have provided a significant breakthrough in this regard.[4] These hybrid materials have extremely high surface areas and pore volumes, uniform pore sizes, and chemical functionalities.[5] Moreover, their pore sizes and chemical functionalities can be tuned by modifying the metal group or organic linker.[6,7] Hence, MOFs have attracted considerable interest for their possible use in a variety of applications.[8−10]

The practical use of MOFs in many industrial applications such as natural gas sweetening hinges on the framework stability under harsh conditions such as high pressures up to 60 bar[11] and stability upon exposure to water vapor and acid gases.[12] Novel MOFs are appearing at a very rapid pace,[9] and a few water-stable examples have emerged recently. Cavka et al. was first to synthesize a zirconium(IV)-based MOF (UiO-66) with exceptional stability.[13] This stability has been attributed to the highly oxophilic nature of zirconium(IV), leading to the formation of a very stable inorganic brick $[Zr_6O_4(OH)_4]$. These Zr_6-octahedra are bound to twelve 1,4-benzenedicarboxylic acid (BDC) ligands (each Zr atom is 8-coordinated) leading to a 3D arrangement of micropores (6 Å). In 2010, Cohen et al.[3] first reported the synthesis of amino-, bromo-, nitro-, and naphthalene-functionalized UiO-66 MOFs. Later in the same year, Kandiah et al.[14] reported that amino-, bromo-, and nitro-functionalized UiO-66 MOFs also retain high thermal and chemical stabilities similar to the parent material. Cmarik et al.[15] observed high stability in other UiO-66 variants including methoxy and naphthyl functional groups. Hence, the UiO-66 framework is quite robust and is exceedingly open to isoreticular functionalization without losing its high hydrothermal and chemical stabilities.

Received: December 2, 2012
Revised: March 4, 2013
Published: March 7, 2013

dx.doi.org/10.1021/jp311857e | J. Phys. Chem. C 2013, 117, 7062−7068

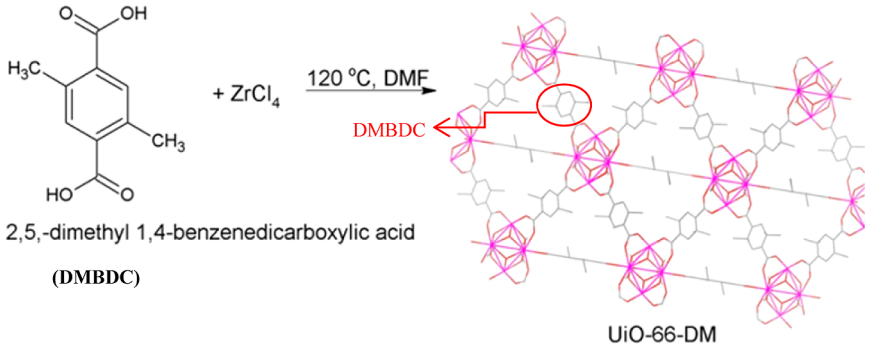

Figure 1. Synthesis of dimethyl-functionalized UiO-66 (UiO-66-DM).

Schoenecker et al. showed that UiO-66 is quite hydrophilic, i.e., it adsorbs a large amount of water vapor at 90% RH (22.42 mmol/g), which is higher than the water adsorption capacities of traditional adsorbents such as zeolites 5A and 13X and BPL carbon.[16] Hence, the UiO-66 framework will be most effective for use in separations under humid conditions only when its affinity for water is reduced; otherwise, the pores will fill with water vapor, thus reducing the adsorption capacity of the target gases, e.g., CO_2 capture from flue gas/natural gas streams. The pore properties and host−guest interactions (hydrophilicity in case of water) can be systematically tuned in MOFs through presynthesis ligand functionalization or postsynthetic modification (PSM). Thus, their adsorption capacity and selectivity toward a targeted gas can be enhanced.

The idea of incorporating hydrophobic functional groups into a MOF structure to reduce water adsorption has been suggested in many literature reports.[15,17−22] However, only a few of these reports have examined CO_2 and CH_4 adsorption as well. Ideally, functionalized MOFs should enhance the adsorption of the target gas without also enhancing the adsorption of water vapor and other mixture components. Cmarik et al.[15] evaluated CO_2, CH_4, N_2, and water vapor adsorption in several variants of UiO-66. The nonpolar naphthyl-functionalized material was found to suppress water adsorption compared to the parent MOF, but the CO_2 loadings were also lowered. Cai et al.[22] studied the adsorption capacity of CO_2 and CH_4 on the alkyl-functionalized MOFs CuMBTC and CuEBTC, with respect to CuBTC or HKUST-1, and found that while water adsorption is significantly lower, the CO_2 loadings at low pressure were unaffected.

Here we report a detailed experimental study of CO_2, CH_4, and water vapor adsorption on a new dimethyl-functionalized version of UiO-66 (UiO-66-DM, Figure 1). This MOF was developed simultaneously by Huang et al.,[23] and our procedure is distinct from their report. In their work, the water effect on the structure was only qualitatively examined, and no CH_4 adsorption data were reported. For comparison with UiO-66-DM, we have also reproduced adsorption isotherms for UiO-66 (Figures 3 and 5). Water vapor adsorption isotherms (Figure 3) at 298 K were measured up to 90% RH, and the gas adsorption isotherms at different temperatures (293−308 K, Figures 5 and S14−16, SI) were measured up to 20 bar. The results show that upon functionalization with hydrophobic dimethyl moieties, water vapor adsorption has been reduced by almost 50% compared to the parent material. In fact, the water adsorption loading is now even less than the water vapor loadings for commercial adsorbents such as zeolites 5A and 13X.[16] Moreover, as expected, this functionalization does not render any adverse effect on the high hydrothermal, chemical, and mechanical stability of the UiO-66 framework (Figures S7−S11, SI). At high pressures (>5 bar) UiO-66-DM has better CO_2/CH_4 selectivity compared to UiO-66, which is promising for natural gas sweetening processes where operating pressures can reach up to 60 bar.

2. EXPERIMENTAL SECTION

2.1. MOF Synthesis. All of the employed chemicals were commercially available and used as received without further purification from the following sources: Sigma-Aldrich, *N*,*N*′-dimethylformamide (DMF); TCI America, 2,5-dimethyl 1,4-benzenedicarboxylic acid (DMBDC); Acros, zirconium(IV) chloride ($ZrCl_4$), 1,4-benzenedicarboxylic acid (BDC).

UiO-66. UiO-66 was synthesized and activated as reported by Schoenecker et al.[16]

UiO-66-DM. Synthesis of UiO-66-DM was performed by using a slightly modified procedure of Lillerud et al.[13] reported for the parent UiO-66 MOF. UiO-66-DM was synthesized by dissolving 0.681 mmol of zirconium(IV) chloride ($ZrCl_4$) and 0.681 mmol of 2,5-dimethyl-1,4-benzenedicarboxylic acid (DMBDC) in 26.5 mL of DMF at room temperature. The resulting mixture was divided equally into two 20 mL scintillation vials. These vials were kept in a sand bath inside an oven at 393 K for 24 h. The final product was cooled to room temperature and then washed with DMF three times to remove the unreacted reactants before activation at 473 K. Similar to the parent material, UiO-66-DM crystallizes as intergrown crystals that are too small for structure determination by single crystal diffraction.

2.2. Characterization. Successful synthesis of UiO-66-DM was confirmed by using ^1H nuclear magnetic resonance (NMR), Fourier transform infrared (FT-IR) spectroscopy, thermogravimetric analysis (TGA) followed by mass spectroscopy (MS), powder X-ray diffraction (PXRD), and N_2 adsorption. Refer to the Supporting Information for more details.

2.3. Water Vapor Adsorption Isotherm Measurements. An Intelligent Gravimetric Analyzer (IGA-3 series, Hiden Analytical Ltd.) was used to obtain water vapor adsorption isotherms. A sample size of approximately 45 mg was used for collecting the water vapor adsorption isotherm. Dry air was used as the carrier gas, with a percentage of it being bubbled through a vessel filled with deionized water. Two mass flow controllers were used to vary the ratio of saturated air and dry air so that the relative humidity (RH) could be controlled. Due to water condensation in the equipment at higher humidities, experiments were conducted up to 90% RH. The

dx.doi.org/10.1021/jp311857e | J. Phys. Chem. C 2013, 117, 7062−7068

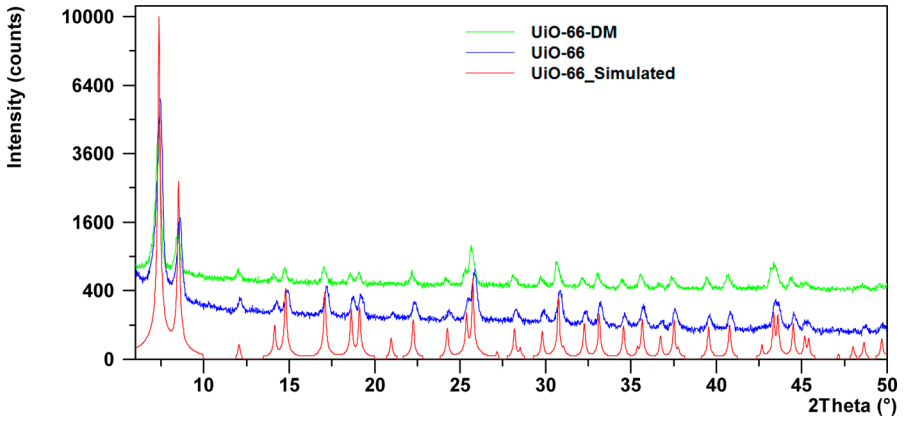

Figure 2. Comparison between PXRD patterns of as-synthesized UiO-66-DM, UiO-66, and the theoretical pattern of UiO-66 simulated from single crystal data.

total gas flow rate was set at 200 cm^3/min, and each adsorption/desorption step was allowed enough time (maximum time of 24 h) to approach equilibrium. UiO-66-DM was activated in situ under vacuum at 473 K for 12 h to remove residual solvent molecules before starting the adsorption measurements. UiO-66-DM was regenerated by heating at 473 K under vacuum for 12 h after the water adsorption isotherm measurement and prior to PXRD and BET analysis.

2.4. High-Pressure Gas Adsorption Isotherm Measurements. An Intelligent Gravimetric Analyzer (IGA-1 series, Hiden Analytical Ltd.) was used to collect pure gas (CO_2 and CH_4) adsorption isotherms at various temperatures (293−308 K, Figures S14−16, SI) and pressures up to 20 bar. UiO-66-DM was activated in situ at 473 K under vacuum until no further weight loss was observed. After activation, the system was maintained under vacuum, and the temperature was adjusted to the desired value. A sample size of approximately 30 mg was used for the measurements, and a maximum equilibration time of 30 min was used for each point in the isotherm.

3. RESULTS AND DISCUSSION

3.1. Structure Characterization and Physical Properties. The PXRD pattern obtained for the as-synthesized UiO-66-DM is compared with the pattern simulated from the single-crystal structure of UiO-66 in Figure 2. These patterns are consistent with each other, confirming that UiO-66-DM has the same topology as the parent UiO-66. Evidence of the presence of the dimethyl moieties on the BDC linker was obtained by characterizing the UiO-66-DM with ^1H NMR and FTIR spectroscopy. The ^1H NMR spectrum of activated (under vacuum at 473 K, 12 h) UiO-66-DM displayed resonances associated with the DMBDC ligand (Figure S1, SI). The peak at 1650 cm^{-1} in the FTIR pattern corresponds to C═O in DMF/DEF.[24] Figure S2 in the SI shows peaks at 1660 and 3430 cm^{-1} in the FTIR spectrum of as-synthesized UiO-66-DM, which corresponds to C═O in DMF and O−H in both the inorganic brick $[Zr_6O_4(OH)_4]$ and physisorbed water, respectively. Hence, an absence of the peak at 1650 cm^{-1} in the FTIR spectrum of activated UiO-66-DM (Figure S3, SI) confirms the removal of DMF molecules after activation. Moreover, the peak at 3430 cm^{-1} has also disappeared for activated UiO-66-DM (Figure S3, SI), which confirms the removal of physisorbed water and dehydroxylation of the $Zr_6O_4(OH)_4$ cornerstone (each Zr atom is 8-coordinated) into Zr_6O_6 (each Zr atom is 7-coordinated) during activation. However, Figure S3 in the SI is now showing a peak at ∼3680 cm^{-1}, which also represents OH-groups on the $Zr_6O_4(OH)_4$ corner stone. However, the intensity of this peak is small. This is consistent with the observation made by Valenzano et al. for the parent UiO-66.[25] Thus, heating the as-synthesized UiO-66-DM at 473 K under vacuum is appropriate for activation. Furthermore, a peak is observed at 2930 cm^{-1} that corresponds to the stretching frequency of the C−H bond in the dimethyl moieties attached to the benzene ring. Hence, FTIR also confirms the presence of DMBDC ligand in this MOF.

The thermal stability of UiO-66-DM was examined by using TGA. The decomposition during the TGA experiment was followed by mass spectrometry (MS). Figure S4 in the SI shows that UiO-66-DM decomposes at approximately 723 K, which is less than the reported decomposition temperature of UiO-66 (813 K)[13] but still higher than the typical value of 623 K observed for many other MOFs.[13] Dingemans et al.[18] synthesized methyl-functionalized MOF-5, and also observed a similar decrease in the thermal stability. UiO-66-NH_2 and UiO-66-NO_2 have also been shown to decompose at a lower temperature compared to UiO-66.[14] However, the origin of the differences in these thermal stabilities is still unclear. Similar to UiO-66,[25] the TGA curve for as-synthesized UiO-66-DM in Figure S4 (SI) shows three weight loss regions before framework decomposition that corresponds to dehydration (physisorbed water, $T < 373$ K), solvent removal (DMF, 373 K $< T <$ 453 K), and dehydroxylation of the $Zr_6O_4(OH)_4$ cornerstone into Zr_6O_6 (453 K $< T <$ 553 K).

In Figure S5 (SI), around the decomposition temperature of UiO-66-DM, we see MS signals mainly due to CO_2 (at m/z values of 12, 28, 44) and *p*-xylene (at m/z values of 91, 106). This suggests bond cleavage between the linker and the inorganic brick as well as cleavage of the bond between the *p*-xylene ring and the terminal carboxyl groups. The absence of an MS signal for DMF (at m/z values of 38, 42, 73) confirms that heating the as-synthesized UiO-66-DM at 473 K under vacuum is appropriate for activation. We also observe a weight loss in the temperature range of 473−573 K at an m/z value of 18 due to release of water for the activated sample. This shows that the activated material rehydroxylates or physisorbs water upon exposure to moisture present in the air during the transfer of the sample to the TGA system. Wiersum et al.[26] also showed that activated/dehyroxylated UiO-66 rehydroxylates upon exposure to water vapor.

dx.doi.org/10.1021/jp311857e | J. Phys. Chem. C 2013, 117, 7062−7068

As expected, N_2 adsorption (Figure S12) at 77 K on the activated UiO-66-DM sample shows that functionalization by the dimethyl moieties leads to reduced porosity (Table 1)

Table 1. Adsorption Loadings at 90% Relative Humidity and BET Surface Areas Before and After Water Exposure

				surface area[a] (m^2/g)		
material	pore vol[b] (cm^3/g)	pore diameter (Å)	loading, 90% RH (cm^3 H_2O/g)	before	after	% loss
UiO-66[c]	0.52	~6	0.43	1160	1136	2
UiO-66-DM	0.40	<6	0.24	811	797	2

[a]BET analysis. [b]Obtained from the Dubinin–Astakov model of N_2 adsorption at 77 K. [c]Reported from ref 16.

compared to the parent MOF. The BET surface area of UiO-66-DM is calculated to be 811 m^2/g, with a DA pore volume of 0.40 cm^3/g. Entry to the internal pores of the parent UiO-66 MOF is limited by triangular windows of 6 Å.[13] However, in UiO-66-DM, functionalization by the dimethyl moieties should further reduce the window opening.

3.2. High Structural Stability. The sensitivity of MOFs under humid conditions is well known, but water adsorption studies on MOFs are still lacking compared to other adsorbates.[21,27−31] Recently, we measured the water vapor adsorption isotherms of several well-known MOFs including UiO-66 and its several variants and found that this family of MOFs is uniformly stable in the presence of water.[15,16] In the current study, water vapor adsorption measurements for UiO-66-DM and subsequent stability tests were performed to compare with UiO-66.

In Figure 3, UiO-66-DM shows significantly lower water adsorption loadings compared to UiO-66 and is also even lower

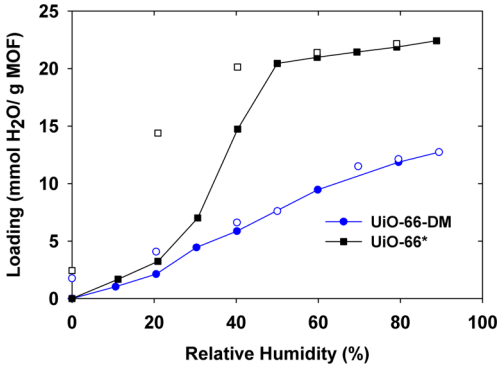

Figure 3. Comparison of water vapor adsorption isotherms at 298 K for the desolvated compounds UiO-66-DM and UiO-66 (closed symbols: adsorption; open symbols: desorption). An asterisk indicates values obtained from our previous work (ref 16).

than the water vapor loadings for traditional porous materials such as zeolites 5A and 13X and BPL carbon.[16] Among the UiO-66 variants studied by Cmarik et al.,[15] the naphthyl-functionalized MOF displayed the lowest water adsorption loadings but still adsorbed approximately 13 mmol/g at 40% RH compared to only 6 mmol/g adsorbed in UiO-66-DM under the same conditions. The desorption isotherms of these Zr-MOFs exhibit hysteresis with a portion of the water being retained. At 0% RH, UiO-66 and UiO-66-DM retain 2.42 and 1.75 mmol/g, respectively. For comparison, UiO-66-NO_2 was shown to retain almost 6 mmol/g of water after desorption,[15] and UiO-66-NH_2 retains approximately 3.3 mmol/g.[16] Wiersum et al.[26] showed that the amount of water retained by UiO-66 after the first adsorption cycle corresponds to partial rehydroxylation of the sample, and full rehydroxylation was possible only after the third cycle. Thus, the same explanation of partial rehydroxylation can be extended to the functionalized UiO-66 MOFs as well. However, we do expect a different extent of rehydroxylation to occur after the first cycle for UiO-66-NO_2, −NH_2, and −DM compared to UiO-66 because the amount retained at 0% RH appears to be related to the polarity or hydrophilicity of the functional group. Thus, the amount of water retained in the MOFs at 0% RH follows the trend UiO-66-NO_2 > −NH_2 > −DM ~ −naphthyl ~ parent structure.

PXRD patterns for UiO-66-DM before and after water exposure are shown in Figure 4. Similar to the previously

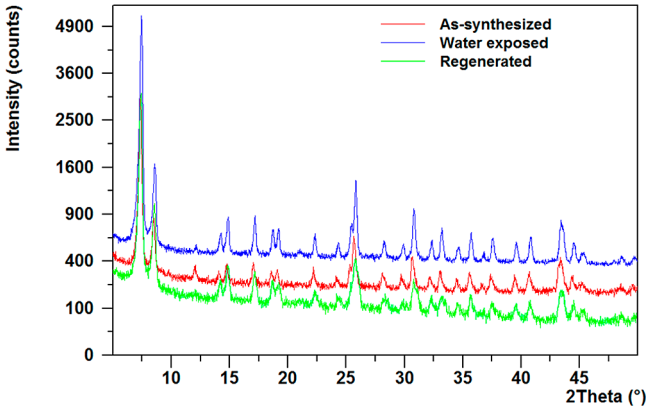

Figure 4. PXRD patterns for as-synthesized (middle), water vapor-exposed (top), and regenerated (bottom) UiO-66-DM.

studied variants,[15,16] UiO-66-DM also does not lose its crystallinity and is quite robust as there is negligible loss in its BET surface area (shown in Table 1) even after exposure to high levels of humidity. Moreover, functionalization with dimethyl moieties does not render any adverse effect on the high chemical and mechanical stability of the framework (Figures S8−S11, SI), in spite of the slightly lower thermal stability. The volumetric water loadings (cm^3/g) at 90% RH are shown in Table 1. It is expected that water should completely fill the pores at saturation, but for UiO-66, the water volume is slightly lower than the pore volume obtained from nitrogen adsorption. This may be due to the fact that only during water adsorption does the Zr inorganic unit undergo rehydroxylation from $[Zr_6O_6]$ to $[Zr_6O_4(OH)_4]$. Thus, it is difficult to directly compare pore volumes obtained from water adsorption with those obtained by N_2 adsorption. The water volume obtained for UiO-66-DM is 40% lower than the pore volume obtained by N_2 adsorption. Similar to UiO-66, this decrease in volume relative to the N_2 pore volume will have contributions from the rehydroxylation process. However, adsorption saturation has not been reached at 90% RH, so water does not fully fill the pores of UiO-66-DM. Thus, the volume should be much lower than the N_2 volume.

Zeolite 13X has often been employed commercially for CO_2 separation from gas streams due to its high CO_2 adsorption capacity under dry conditions, but also must be regenerated at high temperature (623 K) to retain this capacity and has a high affinity for moisture.[32,33] Counter to this, UiO-66-DM can be

dx.doi.org/10.1021/jp311857e | J. Phys. Chem. C 2013, 117, 7062−7068

regenerated at relatively lower temperatures (473 K). Moreover, at 28% RH zeolite 13X[32] adsorbs 15.11 mmol H_2O/g which is ~3.5 times more than the water adsorption in UiO-66-DM at 30% RH. Since the pore volume and surface area of zeolite 13X (0.25 cm^3/g, 725 m^2/g)[34,35] are lower than UiO-66-DM (Table 1), we expect UiO-66-DM to have a higher capacity for gases such as CO_2 at higher pressures and outperform zeolite 13X, especially under humid environments. Water adsorption studies on other MOFs, e.g. the DMOF or Zn-BDC-DABCO family,[36,37] also show much lower water loadings than zeolite 13X, but many of these MOFs lose their crystallinity after exposure to humidity, with the exception of the tetramethyl and anthracene derivatives. In general, the key to developing high-performance adsorbents is finding a balance between adsorption capacity and selectivity for the target; these two characteristics are often inversely related.

3.3. CO_2 and CH_4 Adsorption. Inspired by the high stability and significantly low water loadings of UiO-66-DM, pure-component CO_2 and CH_4 adsorption isotherms were measured. The CO_2 and CH_4 adsorption isotherms for UiO-66 and UiO-66-DM shown in Figure 5 exhibit type I isotherms with no hysteresis. CO_2 is more strongly adsorbed than CH_4 because it has a relatively high quadrupole moment while CH_4 is nonpolar. At high pressure (Figure 5a), the adsorption loadings are higher for the parent material since it has a higher pore volume. However, Figure 5b shows that CO_2 and CH_4 loadings at low pressures are slightly enhanced in UiO-66-DM due to the presence of increased van der Waals interactions from the dimethyl moieties; the enhancement is relatively greater for CH_4 than CO_2. This can be more easily seen by comparing the values of Henry's constants (K_H) for CH_4 and CO_2 adsorption on UiO-66-DM and UiO-66 in Table 2. The Toth parameters (eq S1, SI)[38] were used to calculate Henry's constants. Results show that functionalization with dimethyl moieties leads to an increase in the value of K_H (Table 2) by a factor of 2 for CO_2 and a factor of 3 for CH_4 compared to the parent MOF. This is disadvantageous from the CO_2/CH_4 selectivity point of view in the low-pressure region. These results are different than the behavior observed for UiO-66-naphthyl where the Henry's constant is essentially unchanged compared to the parent material.[15] Steric factors are clearly at play in these examples since the BDC in UiO-66-DM is functionalized on both sides of the benzene ring and on one side for UiO-66-naphthyl.

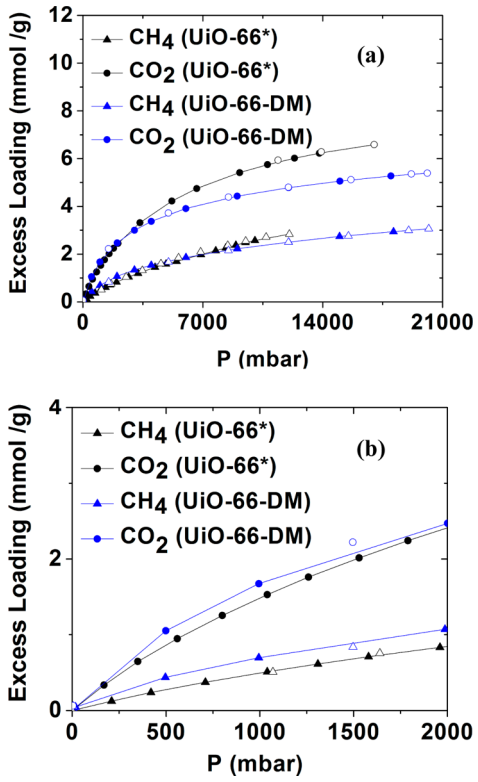

Figure 5. Experimental adsorption−desorption isotherms for CO_2 and CH_4 in UiO-66, and UiO-66-DM at 303 K (closed symbols: adsorption; open symbols: desorption): (a) 0−20 000 mbar and (b) 0−2000 mbar. Lines connecting the adsorption points are to faciliate viewing. An asterisk indicates values reported from ref 26.

The ideal adsorbed solution theory (IAST)[39] has been applied to calculate CO_2/CH_4 selectivity for an equimolar mixture at 303 K in UiO-66 and UiO-66-DM (Figure 6). Up to

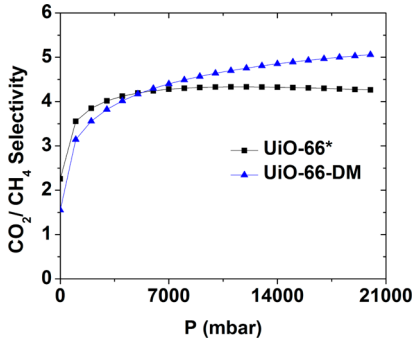

Figure 6. CO_2/CH_4 selectivity for equimolar CO_2/CH_4 gas mixture in UiO-66, and UiO-66-DM at 303 K, calculated by using IAST. Lines connecting the points are to faciliate viewing. An asterisk shows pure component excess loading data for CO_2 and CH_4 adsorption in UiO-66 taken from ref 26.

5000 mbar, the CO_2 selectivity over CH_4 is higher in UiO-66, but above 5000 mbar, UiO-66-DM has the higher selectivity. At low pressure, CH_4 molecules are adsorbed in the tetrahedral cages of UiO-66-DM at a larger concentration compared to CO_2 due to enhanced van der Waals interactions with the dimethyl moieties. However, in UiO-66 under the same conditions, a larger concentration of CO_2 molecules is adsorbed in the tetrahedral cages.[40] Now, when pressure increases

Table 2. Toth Equation Parameters, Henry's Constants (K_H), and Low Coverage CO_2/CH_4 Selectivities at 303 K for UiO-66 and UiO-66-DM

	CO_2			CH_4					
MOF	N_s	b	t	N_s	b	t	$K_H^{CO_2} = N_s b$ (mmol/g.mbar)	$K_H^{CH_4} = N_s b$ (mmol/g.mbar)	ideal selectivity $K_H^{CO_2}/K_H^{CH_4}$
UiO-66	10.11	2.06×10^{-04}	0.76	42.95	2.28×10^{-05}	0.35	2.08×10^{-03}	9.78×10^{-04}	2.12
UiO-66-DM	07.71	4.92×10^{-04}	0.61	10.53	2.58×10^{-04}	0.36	3.79×10^{-03}	2.72×10^{-03}	1.39

dx.doi.org/10.1021/jp311857e | J. Phys. Chem. C 2013, 117, 7062−7068

beyond 5000 mbar, the CO_2/CH_4 selectivity is higher for UiO-66-DM because of the competitive adsorption behavior in which adsorbed CO_2 molecules push CH_4 molecules to the octahedral cages. Good CO_2/CH_4 selectivity at high pressure is advantageous for processes such as natural gas sweetening where the operating pressure can range up to 60 bar.[11] Cu-BTC has been shown to have a higher CO_2/CH_4 selectivity (5−9 for 50:50 CO_2/CH_4 mixture)[41] compared to UiO-66-DM, but water adsorbs strongly in Cu-BTC, and it is eventually unstable under humid conditions. CO_2/CH_4 selectivity of UiO-66-DM at high pressures is comparable to other well-known MOFs such as MIL-53 (Al, Cr).[42,43]

The isosteric heat of adsorption was calculated by applying the Clausius−Clapeyron equation (eq S2, SI)[38] to adsorption isotherms measured at three temperatures (Figures S14 and 15, SI). The isosteric heats of adsorption (Figure 7) calculated for

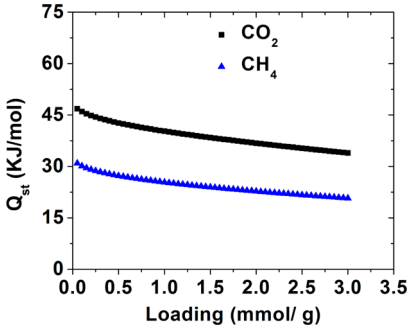

Figure 7. Isosteric heat of adsorption for CO_2 and CH_4 in UiO-66-DM as a function of adsorbate loading. Q_{st} is calculated by using the Clausius−Clapeyron equation.

CH_4 and CO_2 on UiO-66-DM at a loading of 0.05 mmol/g are 30.9 and 46.8 kJ/mol, respectively. These values are quite high compared to UiO-66 and its other functionalized versions.[15,40,44] The high stability of UiO-66-DM, low interaction with water, and good CO_2/CH_4 selectivity at high pressures compared to UiO-66 make it a promising adsorbent for adsorption separations at these conditions.

4. CONCLUSION

In summary, the synthesis and characterization of a new water resistant, highly robust dimethyl-functionalized UiO-66 analogue (UiO-66-DM) has been carried out. Our study shows that functionalization by dimethyl moieties significantly reduces the water loading by almost a factor of 2 compared to UiO-66 without altering the high stability of the framework. Moreover, the water adsorption loadings and regeneration temperature of UiO-66-DM are significantly lower than the benchmark material zeolite 13X. UiO-66-DM also performs better than the parent MOF for CO_2/CH_4 separation at high pressures. While amine groups have been a topic of intense focus for CO_2 separations, this work shows that nonpolar functional groups may also play an important role in enhancing CO_2 adsorption while lowering interactions with water. UiO-66-DM has low affinity for water, is highly robust, and has a good CO_2/CH_4 selectivity at high pressures. In general, understanding the trade-offs between water adsorption behavior and high selectivity and high capacity for the target will be key to developing new adsorbents for CO_2 capture.

■ ASSOCIATED CONTENT

Supporting Information

^1H NMR spectrum, FT-IR spectra, TG-MS curves, PXRD patterns, and N_2 adsorption data. This material is available free of charge via the Internet at http://pubs.acs.org.

■ AUTHOR INFORMATION

Corresponding Author

*E-mail: krista.walton@chbe.gatech.edu. Fax: +1-404-894-2866. Tel: +1-404-894-5254.

Notes

The authors declare no competing financial interest.

■ ACKNOWLEDGMENTS

This material is based upon work supported by Army Research Office PECASE Award W911NF-10-1-0079 and Contract W911NF-10-1-0076.

■ REFERENCES

(1) Davis, M. E. Ordered Porous Materials for Emerging Applications. *Nature* **2002**, *417*, 813−821.
(2) Ferey, G. Hybrid Porous Solids: Past, Present, Future. *Chem. Soc. Rev.* **2008**, *37*, 191−214.
(3) Garibay, S. J.; Cohen, S. M. Isoreticular Synthesis and Modification of Frameworks with the UiO-66 Topology. *Chem. Commun.* **2010**, *46*, 7700−7702.
(4) Ferey, G.; Mellot-Draznieks, C.; Serre, C.; Millange, F. Crystallized Frameworks with Giant Pores: Are There Limits to the Possible? *Acc. Chem. Res.* **2005**, *38*, 217−225.
(5) Li, J.-R.; Kuppler, R. J.; Zhou, H.-C. Selective Gas Adsorption and Separation in Metal-Organic Frameworks. *Chem. Soc. Rev.* **2009**, *38*, 1477−1504.
(6) Eddaoudi, M.; Kim, J.; Rosi, N.; Vodak, D.; Wachter, J.; O'Keeffe, M.; Yaghi, O. M. Systematic Design of Pore Size and Functionality in Isoreticular MOFs and Their Application in Methane Storage. *Science* **2002**, *295*, 469−472.
(7) Karra, J. R.; Walton, K. S. Effect of Open Metal Sites on Adsorption of Polar and Nonpolar Molecules in Metal-Organic Framework Cu-BTC. *Langmuir* **2008**, *24*, 8620−8626.
(8) Keskin, S.; Van Heest, T. M.; Sholl, D. S. Can Metal-Organic Framework Materials Play a Useful Role in Large-Scale Carbon Dioxide Separations? *ChemSusChem* **2010**, *3*, 879−891.
(9) Keskin, S.; Kizilel, S. Biomedical Applications of Metal Organic Frameworks. *Ind. Eng. Chem. Res.* **2011**, *50*, 1799−1812.
(10) Kitagawa, S.; Kitaura, R.; Noro, S. Functional Porous Coordination Polymers. *Angew. Chem., Int. Ed.* **2004**, *43*, 2334−2375.
(11) Herm, Z. R.; Krishna, R.; Long, J. R. CO_2/CH_4, CH_4/H_2 and $CO_2/CH_4/H_2$ Separations at High Pressures Using Mg_2(dobdc). *Microporous Mesoporous Mater.* **2012**, *151*, 481.
(12) Han, S.; Huang, Y.; Watanabe, T.; Dai, Y.; Walton, K. S.; Nair, S.; Sholl, D. S.; Meredith, J. C. High-Throughput Screening of Metal-Organic Frameworks for CO_2 Separation. *ACS Comb. Sci.* **2012**, *14*, 263−267.
(13) Cavka, J. H.; Jakobsen, S.; Olsbye, U.; Guillou, N.; Lamberti, C.; Bordiga, S.; Lillerud, K. P. A New Zirconium Inorganic Building Brick Forming Metal Organic Frameworks with Exceptional Stability. *J. Am. Chem. Soc.* **2008**, *130*, 13850−13851.
(14) Kandiah, M.; Nilsen, M. H.; Usseglio, S.; Jakobsen, S.; Olsbye, U.; Tilset, M.; Larabi, C.; Quadrelli, E. A.; Bonino, F.; Lillerud, K. P. Synthesis and Stability of Tagged UiO-66 Zr-MOFs. *Chem. Mater.* **2010**, *22*, 6632−6640.
(15) Cmarik, G. E.; Kim, M.; Cohen, S. M.; Walton, K. S. Tuning the Adsorption Properties of UiO-66 via Ligand Functionalization. *Langmuir* **2012**, *28*, 15606−15613.
(16) Schoenecker, P. M.; Carson, C. G.; Jasuja, H.; Flemming, C. J. J.; Walton, K. S. Effect of Water Adsorption on Retention of Structure

and Surface Area of Metal−Organic Frameworks. *Ind. Eng. Chem. Res.* **2012**, *51*, 6513−6519.
(17) Wu, T.; Shen, L.; Luebbers, M.; Hu, C.; Chen, Q.; Ni, Z.; Masel, R. I. Enhancing the Stability of Metal-Organic Frameworks in Humid Air by Incorporating Water Repellent Functional Groups. *Chem. Commun.* **2010**, *46*, 6120−6122.
(18) Yang, J.; Grzech, A.; Mulder, F. M.; Dingemans, T. J. Methyl Modified MOF-5: A Water Stable Hydrogen Storage Material. *Chem. Commun.* **2011**, *47*, 5244−5246.
(19) Nguyen, J. G.; Cohen, S. M. Moisture-Resistant and Superhydrophobic Metal-Organic Frameworks Obtained via Post-synthetic Modification. *J. Am. Chem. Soc.* **2010**, *132*, 4560−4561.
(20) Paranthaman, S.; Coudert, F.-X.; Fuchs, A. H. Water Adsorption in Hydrophobic MOF Channels. *Phys. Chem. Chem. Phys.* **2010**, *12*, 8123−8129.
(21) Ma, D.; Li, Y.; Li, Z. Tuning the Moisture Stability of Metal-Organic Frameworks by Incorporating Hydrophobic Functional Groups at Different Positions of Ligands. *Chem. Commun.* **2011**, *47*, 7377−7379.
(22) Cai, Y.; Zhang, Y. D.; Huang, Y. G.; Marder, S. R.; Walton, K. S. Impact of Alkyl-Functionalized BTC on Properties of Copper-Based Metal-Organic Frameworks. *Cryst. Growth Des.* **2012**, *12*, 3709−3713.
(23) Huang, Y.; Qin, W.; Li, Z.; Li, Y. Enhanced Stability and CO_2 Affinity of a UiO-66 Type Metal-Organic Framework Decorated with Dimethyl Groups. *Dalton Trans.* **2012**, *41*, 9283−9285.
(24) Mu, B.; Huang, Y.; Walton, K. S. A Metal-Organic Framework with Coordinatively Unsaturated Metal Centers and Microporous Structure. *CrystEngComm* **2010**, *12*, 2347−2349.
(25) Valenzano, L.; Civalleri, B.; Chavan, S.; Bordiga, S.; Nilsen, M. H.; Jakobsen, S.; Lillerud, K. P.; Lamberti, C. Disclosing the Complex Structure of UiO-66 Metal Organic Framework: A Synergic Combination of Experiment and Theory. *Chem. Mater.* **2011**, *23*, 1700−1718.
(26) Wiersum, A. D.; Soubeyrand-Lenoir, E.; Yang, Q.; Moulin, B.; Guillerm, V.; Yahia, M. B.; Bourrelly, S.; Vimont, A.; Miller, S.; Vagner, C.; Daturi, M.; Clet, G.; Serre, C.; Maurin, G.; Llewellyn, P. L. An Evaluation of UiO-66 for Gas-Based Applications. *Chem. Asian J.* **2011**, *6*, 3270−3280.
(27) Greathouse, J. A.; Allendorf, M. D. The Interaction of Water with MOF-5 Simulated by Molecular Dynamics. *J. Am. Chem. Soc.* **2006**, *128*, 10678−10679.
(28) Kaye, S. S.; Dailly, A.; Yaghi, O. M.; Long, J. R. Impact of Preparation and Handling on the Hydrogen Storage Properties of Zn_4O(1,4-benzenedicarboxylate)$_3$ (MOF-5). *J. Am. Chem. Soc.* **2007**, *129*, 14176−14177.
(29) Kondo, A.; Daimaru, T.; Noguchi, H.; Ohba, T.; Kaneko, K.; Kanob, H. Adsorption of Water on Three-Dimensional Pillared-Layer Metal-Organic Frameworks. *J. Colloid Interface Sci.* **2007**, *314*, 422−426.
(30) Li, Y.; Yang, R. T. Gas Adsorption and Storage in Metal-Organic Framework MOF-177. *Langmuir* **2007**, *23*, 12937−12944.
(31) Low, J. J.; Benin, A. I.; Jakubczak, P.; Abrahamian, J. F.; Faheem, S. A.; Willis, R. R. Virtual High Throughput Screening Confirmed Experimentally: Porous Coordination Polymer Hydration. *J. Am. Chem. Soc.* **2009**, *131*, 15834−15842.
(32) Franchi, R. S.; Harlick, P. J. E.; Sayari, A. Applications of Pore-Expanded Mesoporous Silica. 2. Development of a High-Capacity, Water-Tolerant Adsorbent for CO_2. *Ind. Eng. Chem. Res.* **2005**, *44*, 8007−8013.
(33) Cavenati, S.; Grande, C. A.; Rodrigues, A. E. Adsorption Equilibrium of Methane, Carbon Dioxide, and Nitrogen on Zeolite 13X at High Pressures. *J. Chem. Eng. Data* **2004**, *49*, 1095−1101.
(34) Cortes, F. B.; Chejne, F.; Carrasco-Marin, F.; Moreno-Castilla, C.; Perez-Cadenas, A. F. Water Adsorption on Zeolite 13X: Comparison of the Two Methods Based on Mass Spectrometry and Thermogravimetry. *Adsorption* **2010**, *16*, 141−146.
(35) Lee, J. S.; Kim, J. H.; Kim, J. T.; Suh, J. K.; Lee, J. M.; Lee, C. H. Adsorption Equilibria of CO_2 on Zeolite 13X and Zeolite X/Activated Carbon Composite. *J. Chem. Eng. Data* **2002**, *47*, 1237−1242.
(36) Jasuja, H.; Huang, Y.; Walton, K. S. Adjusting the Stability of Metal−Organic Frameworks under Humid Conditions by Ligand Functionalization. *Langmuir* **2012**, *28*, 16874−16880.
(37) Jasuja, H.; Burtch, N. C.; Huang, Y.; Cai, Y.; Walton, K. S. Kinetic Water Stability of an Isostructural Family of Zinc-Based Pillared Metal−Organic Frameworks. *Langmuir* **2012**, *29*, 633−642.
(38) Duong, D. D. In *Adsorption Analysis: Equilibria and Kinetics*; Imperial College Press: London, UK, 1998.
(39) Myers, A. L.; Prausnitz, J. M. Thermodynamics of Mixed-Gas Adsorption. *AIChE J.* **1965**, *11*, 121−127.
(40) Yang, Q. Y.; Wiersum, A. D.; Jobic, H.; Guillerm, V.; Serre, C.; Llewellyn, P. L.; Maurin, G. Understanding the Thermodynamic and Kinetic Behavior of the CO_2/CH_4 Gas Mixture within the Porous Zirconium Terephthalate UiO-66(Zr): A Joint Experimental and Modeling Approach. *J. Phys. Chem. C* **2011**, *115*, 13768−13774.
(41) Hamon, L.; Jolimaitre, E.; Pirngruber, G. D. CO_2 and CH_4 Separation by Adsorption Using Cu-BTC Metal-Organic Framework. *Ind. Eng. Chem. Res.* **2010**, *49*, 7497−7503.
(42) Hamon, L.; Llewellyn, P. L.; Devic, T.; Ghoufi, A.; Clet, G.; Guillerm, V.; Pirngruber, G. D.; Maurin, G.; Serre, C.; Driver, G.; Beek, W. V.; Jolimaître, E.; Vimont, A.; Daturi, M.; Férey, G. R. Co-adsorption and Separation of CO_2−CH_4 Mixtures in the Highly Flexible MIL-53(Cr) MOF. *J. Am. Chem. Soc.* **2009**, *131*, 17490−17499.
(43) Finsy, V.; Ma, L.; Alaerts, L.; De Vos, D. E.; Baron, G. V.; Denayer, J. F. M. Separation of CO_2/CH_4 Mixtures with the MIL-53(Al) Metal−Organic Framework. *Microporous Mesoporous Mater.* **2009**, *120*, 221−227.
(44) Yang, Q.; Wiersum, A. D.; Llewellyn, P. L.; Guillerm, V.; Serred, C.; Maurin, G. Functionalizing Porous Zirconium Terephthalate UiO-66(Zr) for Natural Gas Upgrading: A Computational Exploration. *Chem. Commun.* **2011**, *47*, 9603−9605.